A MICROMECHANICS MODEL FOR THERMOELASTIC PROPERTIES OF WOVEN COMPOSITES

Chen Zuorong[a], Yu Shouwen[a], Feng Xiqiao[a], Zhu Dechao[b]

[a]*Department of Engineering Mechanics, Tsinghua University, Beijing 100084, China*
[b]*Institute of Solid Mechanics, Beijing University of Aeronautics & Astronautics, Beijing 100083, China*

ABSTRACT

A homogenization scheme, which was developed by Chen *et al*. [1] for evaluating the effective elastic constants of composites, is extended to predict the effective thermoelastic constants of woven composites. The coupling effects between thermal and mechanical behavior in different directions are taken into account. The effects of yarn cross-sectional shape and area on the effective thermoelastic constants of composites are investigated. It is shown that both the predictions of in-plane and out-of-plane thermoelastic properties are in good agreement with others' theoretical results and FEA predictions, as well as with experimental results available.

KEYWORDS: woven, composites, thermoelastic properties, micromechanics

1. INTRODUCTION

The relatively low damage resistance and low through-thickness mechanical properties of two-dimensional woven composites have impeded their widespread applications in some key structures in aerospace, marine craft and automobiles. Three-dimensional orthogonal woven composites can provide improved damage resistance and better through-thickness mechanical properties. However, the through-thickness yarns are incorporated into preform during the weaving process, which deteriorates the in-plane mechanical performance. Therefore, it is of great interest to investigate the relationships between the thermomechaincal behaviors and the microstructure of 3-D orthogonal woven composites.

Finite element analysis is a useful approach to predict the thermomechanical properties of textile reinforced composites because of its ability to capture the complexity in microstructure. Nevertheless, analytical or semi-analytical approaches still play an important role in many aspects, particularly in pre-design of new textile composites, optimization of microstructure, and evaluation of structural properties, etc.

The “mosaic model”[2], one-dimensional “fiber undulation model”[3] and the two-dimensional “bridging model”[4], which were firstly developed by Ishikawa and Chou based on the classical laminated plate theory, were extended to examine the in-plane thermal expansion coefficients and thermal bending coefficients of 2-D woven composites [5]. The 2-D fiber crimp model proposed by Naik and Ganesh [6], which is also based on the laminated plate theory but use it locally, was used by Ganesh and Naik [7] to predict the

thermal expansion coefficients of plane weave fabric composites. Hahn and Pandy [8] proposed a micromechanics model to determine the effective thermoelastic properties of plain weave fabric composites under the assumption of uniform strain inside the representative volume element. Nevertheless, there are fewer analytical models developed for investigating the effective thermomechanical behaviors of 3-D fabric composites [9-12].

In this paper, a homogenization scheme, which was developed previously for predicting the effective elastic properties of 3-D braided composites [1], is extended to investigate the linear thermoelastic properties of 3-D orthogonal woven composites. The analysis procedure of present asymptotic homogenization scheme is seemingly similar to Pan et al.'s unit cell modeling approaches [12,13], but a completely new homogenization scheme, which considers the continuity conditions at perfectly bonded interface, is established in present analysis. For this reason, the effective thermoelastic properties of 3-D orthogonal woven composites given in this paper are different from the results given by them.

The homogenization scheme is first formulated by considering an N-layer stratified medium. The exact expressions for the effective thermoelastic properties are obtained. For the case of anisotropic phases, the explicit results to the first order approximation are given. An asymptotic homogenization scheme is presented in section 3. The effective thermoelastic properties of a 3-D orthogonal woven composite are investigated in section 4. Firstly, the asymptotic homogenization scheme is validated by comparing present predictions with others' theoretical and experimental results, then the effects of cross-section shapes of warp and weft yarns and z yarn cross-section area on the thermoelastic constants of 3-D orthogonal woven composites are investigated.

2. Formulation for stratified medium

A stratified material with *N*-layer laminates stacked together is considered.

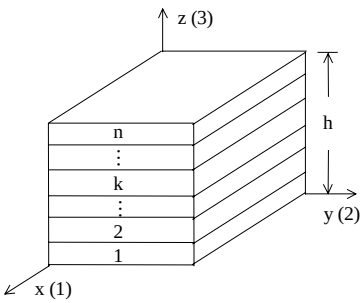

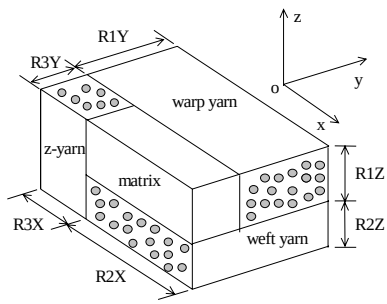

Fig.1. RVE of an N-layer stratified medium. Fig.2. Simplified unit cell geometry model.

The representative volume element (RVE) is shown in Fig.1. Each layer of the material is assumed to be linearly elastic. The thickness of the k-th layer is $h^{(k)}$. The linearly hygrothermoelastic stress-strain relations for the k-th layer can be written as

$$\varepsilon_{ij}^{(k)} = S_{ijpq}^{(k)}\sigma_{pq}^{(k)} + \alpha_{ij}^{(k)}T + \beta_{ij}^{(k)}\theta \qquad (i, j, p, q = 1,2,3; k = 1,2,\mathrm{K}\ , N), \tag{1}$$

where $\varepsilon_{ij}^{(k)}$ is the strain tensor, $\sigma_{ij}^{(k)}$ the stress tensor, $S_{ijpq}^{(k)}$ the elastic compliance tensor,

$\alpha_{ij}^{(k)}$ and $\beta_{ij}^{(k)}$ are the thermal strain tensor and moisture strain tensor, respectively, T and θ the change in the temperature and moisture, respectively.

The stress tensor and the strain tensor can be formally decomposed into two orthogonal complementary parts: the interior part, which is tangential to the interface, and the exterior part, which is normal to the interface. Then Eq.(1) can be expressed using the "in-plane" and the "out-of-plane" components

$$\begin{bmatrix} \boldsymbol{\varepsilon}_t^{(k)} \\ \boldsymbol{\varepsilon}_n^{(k)} \end{bmatrix} = \begin{bmatrix} \boldsymbol{S}_{tt}^{(k)} & \boldsymbol{S}_{tn}^{(k)} \\ \boldsymbol{S}_{nt}^{(k)} & \boldsymbol{S}_{nn}^{(k)} \end{bmatrix} \begin{bmatrix} \boldsymbol{\sigma}_t^{(k)} \\ \boldsymbol{\sigma}_n^{(k)} \end{bmatrix} + \begin{bmatrix} \boldsymbol{\alpha}_t^{(k)} \\ \boldsymbol{\alpha}_n^{(k)} \end{bmatrix} T + \begin{bmatrix} \boldsymbol{\beta}_t^{(k)} \\ \boldsymbol{\beta}_n^{(k)} \end{bmatrix} \theta \qquad (k = 1,2,\mathrm{K}\,,N), \tag{2}$$

where the subscripts t and n indicate the in-plane and out-of-plane components, respectively. It follows from Eq.(2) that

$$\begin{bmatrix} \boldsymbol{\sigma}_t^{(k)} \\ \boldsymbol{\varepsilon}_n^{(k)} \end{bmatrix} = \begin{bmatrix} \boldsymbol{R}_{tt}^{(k)} & \boldsymbol{R}_{tn}^{(k)} \\ \boldsymbol{R}_{nt}^{(k)} & \boldsymbol{R}_{nn}^{(k)} \end{bmatrix} \begin{bmatrix} \boldsymbol{\varepsilon}_t^{(k)} \\ \boldsymbol{\sigma}_n^{(k)} \end{bmatrix} - \begin{bmatrix} \boldsymbol{R}_{tt}^{(k)} & \boldsymbol{0}_{3\times3} \\ \boldsymbol{R}_{nt}^{(k)} & -\boldsymbol{I}_{3\times3} \end{bmatrix} \left\{ \begin{bmatrix} \boldsymbol{\alpha}_t^{(k)} \\ \boldsymbol{\alpha}_n^{(k)} \end{bmatrix} T + \begin{bmatrix} \boldsymbol{\beta}_t^{(k)} \\ \boldsymbol{\beta}_n^{(k)} \end{bmatrix} \theta \right\} \quad (k = 1,2,\mathrm{K}\,,N), \tag{3}$$

where $\boldsymbol{R}_{tt}^{(k)} = \boldsymbol{S}_{tt}^{(k)^{-1}}$, $\boldsymbol{R}_{nt}^{(k)} = -\boldsymbol{R}_{tn}^{(k)^{\mathrm{T}}} = \boldsymbol{S}_{nt}^{(k)} \boldsymbol{S}_{tt}^{(k)^{-1}}$, $\boldsymbol{R}_{nn}^{(k)} = \boldsymbol{S}_{nn}^{(k)} - \boldsymbol{S}_{nt}^{(k)} \boldsymbol{S}_{tt}^{(k)^{-1}} \boldsymbol{S}_{tn}^{(k)}$.

The in-plane components of the strain tensor and the out-of-plane components of the stress tensor must be continuous across the perfectly bonded interface. Thus, it can be assumed that these components in the k-th layer relate to the overall average counterparts in the form

$$\begin{bmatrix} \boldsymbol{\varepsilon}_t^{(k)} \\ \boldsymbol{\sigma}_n^{(k)} \end{bmatrix} = \left[\xi_{ij}(z)\right]_{6\times6} \begin{bmatrix} \overline{\boldsymbol{\varepsilon}}_t \\ \overline{\boldsymbol{\sigma}}_n \end{bmatrix} \qquad (k = 1,2,\mathrm{K}\,,N), \tag{4}$$

where $\overline{\boldsymbol{\varepsilon}}$ and $\overline{\boldsymbol{\sigma}}$ denote the averaged value of $\boldsymbol{\varepsilon}$ and $\boldsymbol{\sigma}$ over the entire RVE, respectively. $\{\xi_{ij}(z)\}$ are continuous and piecewise differentiable functions of z, depending on the states of stress and strain. From Eq. (4), it is followed that

$$\begin{bmatrix} \overline{\boldsymbol{\varepsilon}}_t^{(k)} \\ \overline{\boldsymbol{\sigma}}_n^{(k)} \end{bmatrix} = [\phi]_{6\times6}^{(k)} \begin{bmatrix} \overline{\boldsymbol{\varepsilon}}_t \\ \overline{\boldsymbol{\sigma}}_n \end{bmatrix} \qquad (k = 1,2,\mathrm{K}\,,N). \tag{5}$$

Here, we defined $[\phi]^{(k)}$ as the "mixture concentration factor", which describes the relations between the in-plane components of averaged strain tensor and out-of-plane components of averaged stress tensor in the k-th phase material zone with those of the whole RVE.

By putting Eq.(5) into Eq.(3), it is followed that

$$\begin{bmatrix} \overline{\boldsymbol{\sigma}}_t^{(k)} \\ \overline{\boldsymbol{\varepsilon}}_n^{(k)} \end{bmatrix} = \begin{bmatrix} \boldsymbol{R}_{tt}^{(k)} & \boldsymbol{R}_{tn}^{(k)} \\ \boldsymbol{R}_{nt}^{(k)} & \boldsymbol{R}_{tt}^{(k)} \end{bmatrix} [\phi]^{(k)} \begin{bmatrix} \overline{\boldsymbol{\varepsilon}}_t \\ \overline{\boldsymbol{\sigma}}_n \end{bmatrix} - \begin{bmatrix} \boldsymbol{R}_{tt}^{(k)} & \boldsymbol{0}_{3\times3} \\ \boldsymbol{R}_{tn}^{(k)} & -\boldsymbol{1}_{3\times3} \end{bmatrix} \left\{ \begin{bmatrix} \boldsymbol{\alpha}_t^{(k)} \\ \boldsymbol{\alpha}_n^{(k)} \end{bmatrix} T + \begin{bmatrix} \boldsymbol{\beta}_t^{(k)} \\ \boldsymbol{\beta}_n^{(k)} \end{bmatrix} \theta \right\}$$

$$(k = 1,2,\mathrm{K}\,,N). \tag{6}$$

Correspondingly, the averaged value of $\boldsymbol{\sigma}_t$ and $\boldsymbol{\varepsilon}_n$ can be given as

$$\begin{bmatrix}\overline{\boldsymbol{\sigma}_t}\\ \overline{\boldsymbol{\varepsilon}_n}\end{bmatrix}=\begin{bmatrix}\overline{\boldsymbol{R}}_{tt} & \overline{\boldsymbol{R}}_{tn}\\ \overline{\boldsymbol{R}}_{nt} & \overline{\boldsymbol{R}}_{nn}\end{bmatrix}\begin{bmatrix}\overline{\boldsymbol{\varepsilon}_t}\\ \overline{\boldsymbol{\sigma}_n}\end{bmatrix}-\sum_{k=1}^{N}\mathrm{v}^{(k)}\begin{bmatrix}\overline{\boldsymbol{R}}_{tt}^{(k)} & \boldsymbol{0}\\ \overline{\boldsymbol{R}}_{tn}^{(k)} & -\boldsymbol{1}\end{bmatrix}\left\{\begin{bmatrix}\boldsymbol{\alpha}_t^{(k)}\\ \boldsymbol{\alpha}_n^{(k)}\end{bmatrix}T+\begin{bmatrix}\boldsymbol{\beta}_t^{(k)}\\ \boldsymbol{\beta}_n^{(k)}\end{bmatrix}\theta\right\}, \tag{7}$$

where $\begin{bmatrix}\overline{\boldsymbol{R}}_{tt} & \overline{\boldsymbol{R}}_{tn}\\ \overline{\boldsymbol{R}}_{nt} & \overline{\boldsymbol{R}}_{nn}\end{bmatrix}=\sum_{k=1}^{N}\mathrm{v}^{(k)}\begin{bmatrix}\overline{\boldsymbol{R}}_{tt}^{(k)} & \overline{\boldsymbol{R}}_{tn}^{(k)}\\ \overline{\boldsymbol{R}}_{nt}^{(k)} & \overline{\boldsymbol{R}}_{nn}^{(k)}\end{bmatrix}[\phi]^{(k)}$, and the volume fraction of the k-th phase $\mathrm{v}^{(k)}=h^{(k)}/h$.

Rearrange Eq.(7) into

$$\begin{bmatrix}\overline{\boldsymbol{\varepsilon}_t}\\ \overline{\boldsymbol{\varepsilon}_n}\end{bmatrix}=\begin{bmatrix}\overline{\boldsymbol{S}}_{tt} & \overline{\boldsymbol{S}}_{tn}\\ \overline{\boldsymbol{S}}_{nt} & \overline{\boldsymbol{S}}_{nn}\end{bmatrix}\begin{bmatrix}\overline{\boldsymbol{\sigma}_t}\\ \overline{\boldsymbol{\sigma}_n}\end{bmatrix}+\left\{\begin{bmatrix}\overline{\boldsymbol{\alpha}_t}\\ \overline{\boldsymbol{\alpha}_n}\end{bmatrix}T+\begin{bmatrix}\overline{\boldsymbol{\beta}_t}\\ \overline{\boldsymbol{\beta}_n}\end{bmatrix}\theta\right\}, \tag{8a}$$

where

$$\overline{\boldsymbol{S}}_{tt}=\overline{\boldsymbol{R}}_{tt}^{-1},\ \ \overline{\boldsymbol{S}}_{nt}=\overline{\boldsymbol{S}}_{tn}^{\mathrm{T}}=\overline{\boldsymbol{R}}_{nt}\overline{\boldsymbol{R}}_{tt}^{-1},\ \ \overline{\boldsymbol{S}}_{nn}=\overline{\boldsymbol{R}}_{nn}-\overline{\boldsymbol{R}}_{nt}\overline{\boldsymbol{R}}_{tt}^{-1}\overline{\boldsymbol{R}}_{tn}, \tag{8b}$$

$$\begin{bmatrix}\overline{\boldsymbol{\alpha}_t}\\ \overline{\boldsymbol{\alpha}_n}\end{bmatrix}=\begin{bmatrix}\overline{\boldsymbol{S}}_{tt} & \boldsymbol{0}_{3\times3}\\ \overline{\boldsymbol{S}}_{nt} & -\boldsymbol{1}_{3\times3}\end{bmatrix}\sum_{k=1}^{N}\mathrm{v}^{(k)}\begin{bmatrix}\overline{\boldsymbol{R}}_{tt}^{(k)} & \boldsymbol{0}_{3\times3}\\ \overline{\boldsymbol{R}}_{tn}^{(k)} & -\boldsymbol{1}_{3\times3}\end{bmatrix}\begin{bmatrix}\boldsymbol{\alpha}_t^{(k)}\\ \boldsymbol{\alpha}_n^{(k)}\end{bmatrix}, \tag{8c}$$

$$\begin{bmatrix}\overline{\boldsymbol{\beta}_t}\\ \overline{\boldsymbol{\beta}_n}\end{bmatrix}=\begin{bmatrix}\overline{\boldsymbol{S}}_{tt} & \boldsymbol{0}_{3\times3}\\ \overline{\boldsymbol{S}}_{nt} & -\boldsymbol{1}_{3\times3}\end{bmatrix}\sum_{k=1}^{N}\mathrm{v}^{(k)}\begin{bmatrix}\overline{\boldsymbol{R}}_{tt}^{(k)} & \boldsymbol{0}_{3\times3}\\ \overline{\boldsymbol{R}}_{tn}^{(k)} & -\boldsymbol{1}_{3\times3}\end{bmatrix}\begin{bmatrix}\boldsymbol{\beta}_t^{(k)}\\ \boldsymbol{\beta}_n^{(k)}\end{bmatrix}. \tag{8d}$$

From Eqs.8(a)-(d), the effective linearly hygrothermoelastic stress-strain relations for the stratified material can be written in the form

$$\overline{\varepsilon}_i=\overline{S}_{ij}\overline{\sigma}_j+\overline{\alpha}_iT+\overline{\beta}_i\theta \quad (i,j=1,2,\mathrm{K},6), \tag{9}$$

where $\overline{S}_{ij}$ is the effective elastic compliance tensor, $\overline{\alpha}_i$ and $\overline{\beta}_i$ the effective coefficients of thermal expansion and moisture , respectively.

Up to this point the expressions for the effective thermoelastic properties are obtained. In order to estimate the effective thermoelastic properties of composite materials, the “mixture average concentration factor” have to be determined, which have been the focus of various micromechanics approximations [14]. As a first order approximation, it could be taken as a unity matrix.

For the case of orthotropic phase and the material frame of each phase in accordance with the global coordinates, to the first order approximation, the non-zero elements of $\overline{S}_{ij}$ can be reduced as

$$\overline{S}_{ij}=\sum_{k=1}^{N}\left(\mathrm{v}^{(k)}S_{ij}^{(k)}-\Delta_{11}^{(k)}S_{2i}^{(k)^2}-\Delta_{22}^{(k)}S_{1j}^{(k)^2}+2\Delta_{12}^{(k)}S_{1i}^{(k)}S_{2j}^{(k)}\right)\delta_{ij}+$$

$$\sum_{k=1}^{N}\left(\Delta_{11}^{(k)}S_{2i}^{(k)}-\Delta_{12}^{(k)}S_{1i}^{(k)}\right)\cdot\frac{\sum_{k=1}^{N}\Delta_{12}^{(k)}\sum_{m=1}^{N}\left(\Delta_{22}^{(m)}S_{1j}^{(m)}-\Delta_{12}^{(m)}S_{2j}^{(m)}\right)+\sum_{k=1}^{N}\Delta_{12}^{(k)}\sum_{m=1}^{N}\left(\Delta_{11}^{(m)}S_{2j}^{(m)}-\Delta_{12}^{(m)}S_{1j}^{(m)}\right)}{\sum_{k=1}^{N}\Delta_{11}^{(k)}\sum_{m=1}^{N}\Delta_{22}^{(m)}-\sum_{k=1}^{N}\Delta_{12}^{(k)}\sum_{m=1}^{N}\Delta_{12}^{(m)}}+$$

$$\sum_{k=1}^{N}\left(\Delta_{22}^{(k)}S_{1i}^{(k)}-\Delta_{12}^{(k)}S_{2i}^{(k)}\right)\cdot\frac{\sum_{k=1}^{N}\Delta_{11}^{(k)}\sum_{m=1}^{N}\left(\Delta_{22}^{(m)}S_{1j}^{(m)}-\Delta_{12}^{(m)}S_{2j}^{(m)}\right)+\sum_{k=1}^{N}\Delta_{12}^{(k)}\sum_{m=1}^{N}\left(\Delta_{11}^{(m)}S_{2j}^{(m)}-\Delta_{12}^{(m)}S_{1j}^{(m)}\right)}{\sum_{k=1}^{N}\Delta_{11}^{(k)}\sum_{m=1}^{N}\Delta_{22}^{(m)}-\sum_{k=1}^{N}\Delta_{12}^{(k)}\sum_{m=1}^{N}\Delta_{12}^{(m)}}$$

$$(i,\ j=1,2,3), \qquad (10a)$$

$$\bar{S}_{ij}=\sum_{k=1}^{N}\mathrm{v}^{(k)}S_{ij}^{(k)} \qquad (i=j=4,5), \qquad (10b)$$

$$\bar{S}_{66}=\left(\sum_{k=1}^{N}\mathrm{v}^{(k)}/S_{66}^{(k)}\right)^{-1}, \qquad (10c)$$

where $\Delta_{ij}^{(k)}=\mathrm{v}^{(k)}S_{ij}^{(k)}\left(S_{11}^{(k)}S_{22}^{(k)}-S_{12}^{(k)2}\right)^{-1}$, δ_{ij} is the Kronecker delta.

Correspondingly, the effective coefficients of thermal expansion are

$$\bar{\alpha}_i=\sum_{k=1}^{N}\left(\bar{S}_{1i}-\delta_{i3}S_{1i}^{(k)}\right)\left(\alpha_1^{(k)}\Delta_{22}^{(k)}-\alpha_2^{(k)}\Delta_{12}^{(k)}\right)+ \sum_{k=1}^{N}\left(\bar{S}_{i2}-\delta_{i3}S_{i2}^{(k)}\right)\left(\alpha_2^{(k)}\Delta_{11}^{(k)}-\alpha_1^{(k)}\Delta_{12}^{(k)}\right)+\delta_{i3}\sum_{k=1}^{N}\mathrm{v}^{(k)}\alpha_i^{(k)} \qquad (i=1,2,3.\ \text{no sumon i}). \qquad (10d)$$

The effective elastic properties given by Eqs.10(a)-(c) in the form of compliance constants are as same as the results expressed in the form of stiffness constants [1]. The results given by “X model”, “Y model” and “Z model” can be obtained by neglecting the high order terms in our results.

3.1 A simplified unit cell geometry model for 3-D orthogonal woven composites

3-D orthogonal woven fabrics are generally fabricated by three sets of yarns, i.e., warp, weft and z yarns, which are interlaced in three mutually orthogonal directions. Fig.2 shows a simplified unit cell geometry model, which is commonly used to model the microstructure of 3-D orthogonal woven composites [11-13]. The yarn cross-sectional shapes in the unit cell geometrical model are assumed to be rectangular. The geometry dimensions of yarns, i.e., R1Y and R1Z for warp yarn, R2X and R2Z for weft yarn, R3X and R3Y for z yarn, are shown in Fig.2. The volume fraction of each set of yarns in 3-D orthogonal woven composites can be estimated approximately using the following formulas

$$\mathrm{v}_x=(1+R2Z/R1Z)^{-1}(1+R3Y/R1Y)^{-1}, \qquad (11a)$$

$$\mathrm{v}_y=(1+R1Z/R2Z)^{-1}(1+R3X/R2X)^{-1}, \qquad (11b)$$

$$\mathrm{v}_z=(1+R1Y/R3Y)^{-1}(1+R2X/R3X)^{-1}. \qquad (11c)$$

Where v_x, v_y and v_z denote the volume fraction of warp, weft and z yarns, respectively.

3.2 The asymptotic homogenization scheme

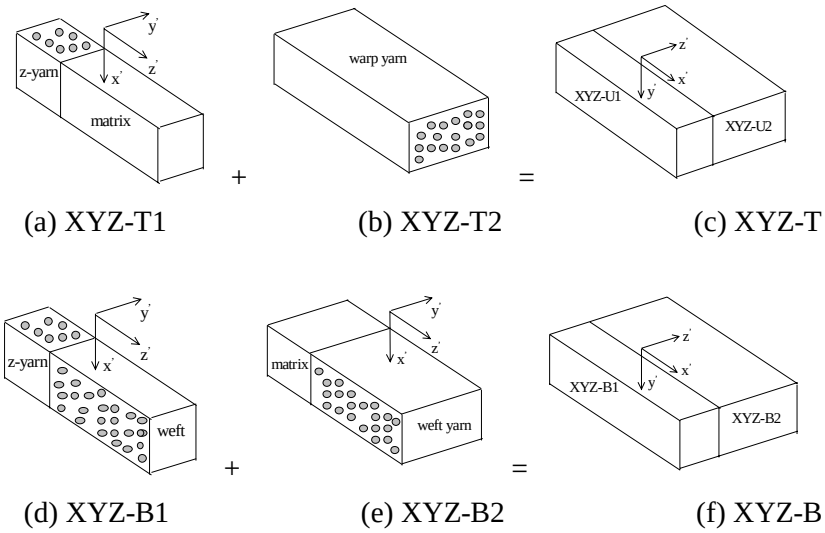

Fig.3. A schematic of “XYZ model” for 3D orthogonal woven composites.

A schematic of “XYZ model” for 3-D orthogonal woven composites is shown in Fig.3. In the modified “XYZ model”, the unit cell [see Fig.2] is divided into four sub-cells, i.e. XYZ-T1, XYZ-T2, XYZ-B1 and XYZ-B2, which are composed of z yarn and matrix, warp yarn, z yarn and weft yarn, and matrix and weft yarn, respectively. The geometrical parameters of each sub-cell can be identified according to the geometry dimensions of the unit cell. The effective thermoelastic constants of sub-cells XYZ-T1, XYZ-B1 and XYZ-B2 can be evaluated using Eqs.10(a)-(d) in their respective local coordinates $x'y'z'$. Then, the effective thermoelastic properties of effective material sub-body XYZ-T can be evaluated by homogenizing sub-cell XYZ-T1 and XYZ-T2 using Eqs.10(a)-(d) again in its local coordinates [see Fig.4(c)]. Similar treatment is applied to the effective material sub-body XYZ-B. Finally, the effective thermoelastic properties of the whole unit cell can be obtained by homogenizing sub-cell XYZ-T and XYZ-B using Eqs.10(a)-(d) once again. As we can see, in the present “XYZ model” the effective thermoelastic properties can be asymptotically obtained by executing the new homogenization scheme firstly in the x direction, then in the y direction and finally in the z direction by using Eqs.10(a)-(d) over again.

4. The effective thermoelastic properties of 3-D orthogonal composites

In this section, comparisons between the present predictions and others' theoretical and experimental results are made to validate the asymptotic homogenization scheme proposed in this paper. Further, the effects of the cross-sectional shapes of warp and weft yarns and z yarn cross-sectional area on the effective thermoelastic properties of 3-D orthogonal woven composites are investigated.

4.1 Validation of the asymptotic homogenization scheme

In order to validate the asymptotic homogenization scheme developed in this paper, comparisons between the present predictions and others' theoretical and experimental results are made.

Table 1. The thermoelastic constants for material constituents [11,12]

	E_1 (GPa)	$E_2 = E_3$ (GPa)	ν_{12} $(=\nu_{13})$	ν_{23}	$G_{12} = G_{13}$ (Gpa)	G_{23} (Gpa)	α_L $(\mu\varepsilon/^{o}C)$	α_T $(\mu\varepsilon/^{o}C)$
yarn	134.0	10.2	0.3	0.49	5.52	3.43	-0.25	27.0
Epoxy resin	3.45	3.45	0.35	0.35	1.28	1.28	69.0	69.0

Table 2. The geometrical parameters for the unit cell [15] (Unit: mm)

	R1Y	R1Z	R2X	R2Z	R3X	R3Y
Unit cell	0.691	0.2335	0.762	0.2235	0.193	0.2235

The elastic constants and coefficients of thermal expansion for the carbon/epoxy yarn and the resin are given in Table 1, while the geometrical parameters for the unit cell of a 3-D orthogonal woven composite are listed in Table 2. Table 3 summaries some results obtained by Tan et al. [12,13] and present predictions. From Table 3, it can be seen that there is a good agreement between the present predictions and Tan et al.'s FEA results, especially for the effective coefficient of thermal expansion α_z.

Table 3. Comparison between the FEA, theoretical models [12,13] and present predictions

Models	E_x (GPa)	E_y (GPa)	E_z (GPa)	G_{xy} (Gpa)	G_{yz} (GPa)	G_{xz} (GPa)	α_x $(\mu\varepsilon/^{o}C)$	α_y $(\mu\varepsilon/^{o}C)$	α_z $(\mu\varepsilon/^{o}C)$
FEA model	57.77	58.24	16.96	4.211	3.54	3.57	5.24	5.18	29.69
XYZ model	57.57	58.23	17.44	4.12	3.68	3.15	5.296	5.233	20.041
Present	57.54	58.18	17.20	3.44	3.67	3.51	5.59	5.43	29.72

Table 4. The geometrical parameters for the unit cell [13]. (Unit: mm)

	R1Y	R1Z	R2X	R2Z	R3X	R3Y
Unit cell	0.691	0.2335	0.762	0.2682	0.193	0.2235

Table 5. Comparison of the predictions and experimental results

Models	E_1 (Gpa)	E_2 (Gpa)	E_3 (Gpa)
Present	53.256	62.718	17.214
FEA model [15]	53.1	62.5	----
Exp. [16]	62.5	72	----

A comparison between the present predictions and the experiment results [16] is carried out also. The elastic constants and coefficients of thermal expansion for the carbon/epoxy yarn and the resin and the geometrical parameters for the unit cell are listed in Table 1 and Table 4, respectively. Comparisons between the present predictions and the corresponding

experimental data [16] are given in Table 5. From the comparison it can be seen that the results predicted by the present homogenization scheme are in good agreement with the FEA results given by Gu et al. [15], and are close to Brandt et al.'s experimental data [16].

4.2 Effects of the cross-sectional shape and area of yarns on thermoelasticities.

To investigate the effects of the cross-sectional shapes of warp and weft yarns, and the cross-sectional area of z yarn on the effective thermoelastic properties of a three-dimensional orthogonal woven composite, five cases were considered here. The thermoelastic properties of the composite constituents listed in Table 1 are used, and the geometrical parameters of the unit cell for the five cases are listed in table 6. For the first three cases, only the cross-sectional shapes of warp and weft yarns are different, then the effects of cross-sectional shape of warp and weft yarns on the effective thermoelastic properties are investigated. While, for the last three cases only the cross-sectional area of z yarn is different, then the effects of cross-sectional area of z yarn on the effective thermoelastic properties are investigated.

Table 6. The geometrical parameters for the unit cell

				Warp yarn		Weft yarn		Z yarn	
Case	v_x (%)	v_y (%)	v_z (%)	R1Y (mm)	R1Z (mm)	R2X (mm)	R2Z (mm)	R3X (mm)	R3Y (mm)
A	33.4	36.6	9.0	0.45	0.45	0.482	0.482	0.2	0.2
B	36.8	39.9	5.4	0.639	0.318	0.681	0.341	0.2	0.2
C	39.1	41.3	3.9	0.78	0.26	0.86	0.27	0.2	0.2
D	37.2	39.5	5.4	0.78	0.26	0.86	0.27	0.25	0.25
E	35.4	37.8	7.2	0.78	0.26	0.86	0.27	0.3	0.3

Table 7. The present predictions

Case	E_x (GPa)	E_y (GPa)	E_z (GPa)	G_{xy} (GPa)	G_{yz} (GPa)	G_{xz} (GPa)	α_x $(\mu\varepsilon/^{o}C)$	α_y $(\mu\varepsilon/^{o}C)$	α_z $(\mu\varepsilon/^{o}C)$
A	51.067	55.226	21.943	3.150	3.716	3.355	7.493	6.557	22.855
B	55.204	59.443	17.752	3.397	3.738	3.429	6.072	5.336	28.733
C	58.074	61.064	16.001	3.569	3.745	3.509	5.240	4.775	32.001
D	55.704	58.779	17.814	3.391	3.721	3.444	6.004	5.442	28.633
E	53.562	56.699	19.790	3.257	3.708	3.400	6.715	6.060	25.595

The predictions by the present "XYZ" homogenization scheme are given in Table 7.

For the case A, B and C, as the aspect ratios of cross sections of warp and weft yarns change from 1:1 in case A to 3:1 in case C, yarn volume fraction v_x and v_y increase and v_z decreases while the total yarn volume fraction still increases, so Young's modulus E_x, E_y and the effective coefficient of thermal expansion α_z increase while E_z, α_x and α_y decrease. This is consistent vith the results reported by Ishikawa et al. [11] and Tan et al. [12] that the effective coefficient of thermal expansion α_x decreases when fiber volume fraction increases. Because of the decrease in v_z, the incrementals of the shear modulus G_{xz} and G_{yz}, which are 4.4% and 0.8%, respectively, is less than that of shear modulus G_{xy}, which is 11.7%. For the case C, D and E, the cross-sectional area of z yarn varies, however the cross-sectional areas of warp

yarn, weft yarn and the aspect ratios of cross sections of all yarns remain constants. The z yarn volume fraction v_z increases while v_x, v_y and the total yarn volume fractions decrease from case C, D to E.

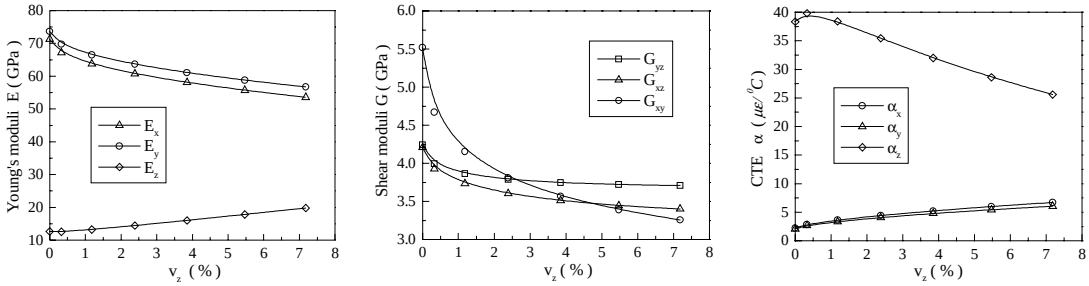

(a) Young's modulus E (b) Shear modulus G (c) Thermal expansion coefficients α

Fig.4 Dependence of effective thermoelastic constants on z yarn volume fraction v_z

The variations of the effective engineering elastic constants E, G and coefficients of thermal expansion α with z yarn volume fraction are shown in Fig.4. From Fig.4 it is can be seen that as the z yarn volume fraction increases, Young's modulu E_z increases while E_x and E_y decrease with the simultaneous decreases in v_x and v_y, shear modulu G_{xy} decreases rapidly for the reason that v_x and v_y simultaneously decrease, while shear modulus G_{xz} and G_{yz} decrease slightly , which is caused by the increase in z yarn wolume fraction. It is noted from Fig.4(c) that as the z yarn volume fraction increases, the effective coefficients of thermal expansion α_x and α_y increase slightly, while α_z increases slightly for small v_z, then decreases significantly for larger v_z. This could be caused by two main reasons. One is that the increase in matrix volume fraction makes α_x, α_y and α_z increase because the coefficient of thermal expansion of matrix, which is 69.0, is larger than those of yarns. The other is that the increase in z yarn volume fraction makes α_x and α_y decrease slightly while α_z decrease rapidly because the transverse and longitudinal coefficients of thermal expansion of yarn, which are 27.0 and –0.25, respectively, are more less than that of matrix.

5 Concluding remarks

An asymptotic homogenization scheme is devoloped to investigate the thermoelastic behaviors of three-dimensional orthogonal woven composites. It is shown that the present predictions are in good agreement with those predicted using related theoretical models and FEA models, and are much closer to the corresponding experimental results available in the literature.

6 ACKNOWLEDGEMENTS

This work is supported in part by the National Natural Science Foundation of China under grant no.19891800, no.19932030 and Fundmental Research Fundation of Tsinghua University under grant no.0611.

References

[1]. Chen ZR, Zhu DC, Lu M, Ye L. "A homogenisation scheme and its application to evaluation of elastic properties of three-dimensional braided composites", *Composites: Part B*, 2001;32(1):67-86.

[2]. Ishikawa T, Chou TW. "Elastic behavior of woven hybrid composites", *Journal of Composite Materials*, 1982;16(1):2-19.

[3]. Ishikawa T, Chou TW. "One-dimensional micromechanical analysis of woven fabric composites", *AIAA Journal*, 1983;21(12):1714-1721.

[4]. Ishikawa T, Chou TW. "Stiffness and strength behavior of woven fabric composites", *Journal of Materials Science*, 1982;17(10):3211-3220.

[5]. Ishikawa T, Chou TW. "In-plane thermal expansion and thermal bending coefficients of fabric composites", *Journal of Composite Materials*, 1983;17(1):92-104.

[6]. Naik NK, Shembekar PS. "Elastic behaviour of woven fabric composites: I-Lamina analysis", *Journal of Composite Materials*, 1992;26(15):2197-2225.

[7]. Naik NK, Ganesh VK. "Analytical method for plain weave fabric composites", *Composites*, 1995:26(4):281-289.

[8]. Hahn HT, Pandy R. "A micromechanics model for thermoelastic properties of plain weave fabric composites", *Journal of Engineering Materials and Technology*, 1994;116(4):517-523.

[9]. Wang YQ, Wang ASD. "Microstructure/property relationships in three-dimensionally braided fiber composites", *Composites Science and Technology*, 1995;53(2):213-222.

[10]. Sankar BV, Marrey RV. "Analytical method for micromechanics of textile composites", *Composites Science and Technology*, 1997;57(6):703-713.

[11]. Ishikawa T, Watanable N, Bansaku K, Ono Y. "Closed form predictions of marcroscopic thermomechanical properties of Orthogonal 3-D woven fabric composites", *Proceedings of the Elecenth International Conference on Composite Materials*, vol.*V*, Gold Coast, Australia, July 14-18, 1997,pp.189-200.

[12]. Tan P, Tong LY, Steven GP. "Models for predicting thermomechanical properties of three-dimensional orthogonal woven composites", *Journal of Reinforced Plastics and Composites*, 1999:18(2):151-185.

[13]. Tan P, Tong LY, Steven GP. "Modeling appriaches for orthogonal woven composites", *Journal of Reinforced Plastics and Composites*, 1998:17(6):545-577.

[14]. Nemat-Nasser S, Hori M. Micromechanics:overproperties of heterogeneous materials, Amsterdam: North-Holland, 1993.

[15]. Gu P, Mohamed M. "Structure and properties of 3-D woven carben/epoxy composites", *ICCM/9*, vol.*IV*, Mardrid, Spain, July 12-16, 1993, pp.568-575.

[16]. Brandt J, Drechsler K, Mohamed M, Gu P. "Manufacture and performance of carbon/epoxy 3-D woven composites". *37th International SAMPE Symposium*, 1992, 9-12 March, 864-877.